Research Article J. Electrochem. Sci. Technol., 2022, 13(3), 369-376

Stability Tests on Anion Exchange Membrane Water Electrolyzer under On-Off Cycling with Continuous Solution Feeding

Atif Khan Niaz[1] and Hyung-Tae Lim[1,2]*

[1]School of Materials Science and Engineering, Changwon National University, Changwon, Gyeongnam 51140, Republic of Korea
[2]Department of Materials Convergence and System Engineering, Changwon National University, Changwon, Gyeongnam 51140, Republic of Korea

ABSTRACT

In this study, the stability of an anion exchange membrane water electrolyzer (AEMWE) cell was evaluated in an on-off cycling operation with respect to an applied electric bias, i.e., a current density of 500 mA cm^{-2}, and an open circuit. The ohmic and polarization resistances of the system were monitored during operation (~800 h) using electrochemical impedance spectra. Specific consideration was given to the ohmic resistance of the cell, especially that of the membrane under on-off cycling conditions, by consistently feeding the cell with KOH solution. Owing to an excess feed solution, a momentary increase in the polarization resistance was observed immediately after the open-circuit. The excess feed solution was mostly recovered by subjecting the cell to the applied electric bias. Stability tests on the AEMWE cell under on-off cycling with continuous feeding even under an open circuit can guarantee long-term stability by avoiding an irreversible increase in ohmic and polarization resistances.

Keywords : Water Electrolysis, Anion Exchange Membrane, Degradation

Received : 25 March 2022, Accepted : 5 May 2022

1. Introduction

According to the Paris agreement (2015), CO_2 emissions should decline to net-zero, and the global rise in temperature should be restricted to ~1.5°C [1-3]. Currently, the percentage use of fossil fuels accounts for approximately 80% of global energy production [4-6]. Research efforts are underway to decrease fossil fuel dependency and develop environmentally friendly systems [4,7]. In this context, power-to-gas (PtG) projects play a vital role in hydrogen production through water electrolysis, where curtailed renewable energy is used [1,8-10]. In water electrolysis, the electric input from renewable energy sources is used to split water into H_2 and O_2. Several technologies are available for water electrolysis, including alkaline water electrolysis (AWE), proton exchange membrane water electrolysis (PEMWE), and anion exchange membrane water electrolysis (AEMWE). The first two are well commercialized, whereas the others are at the research level [11-13]. However, there is growing research interest in AEMWE owing to its potential to compete with PEMWE. High operational current density, inexpensive catalysts, and efficient cell design are some of the distinguishing features of AEMWE. Although PEMWE is a more matured technology, AEMWE still has comparable performance [14]. The main drawback of AEMWE is its lower durability. Several reports point out this deficiency [15-18]. The most important concern is the variables that can affect overall performance. The catalyst employed, operating temperature, feeding solution, static or dynamic conditions, and magnitude of applied bias are some of the variables that directly affect the stability of AEMWE [19-24]. In particular, the on-off operation of AEMWE (simulating renewable energy sources) with an inevitable variable, i.e., the aspect of an open-circuit condition, for example, the nighttime operation of a solar power plant, affect its stability. The electrolyzer cell must be idle in this state. The

*E-mail address: htaelim@changwon.ac.kr

DOI: https://doi.org/10.33961/jecst.2022.00241

open circuit with solution feeding plays a critical role in the stability of AEMWE. The open-circuit condition can be used during AEMWE in the on-off cycling mode. Several studies have been conducted on the static and dynamic operation of AEMWE. However, these studies did not consider the effects of open-circuit conditions and solution feeding [16,22,23,25-29]. The most prominent among these studies was the long-term operation of ~1000 h. Liu et al. conducted AEMWE at a constant current density of 1 A cm^{-2} for > 1000 h. The electrolyzer cell exhibited a slight degradation rate of ~20 μV h^{-1} [29]. Similarly, Carbone et al. conducted AEMWE in dynamic mode with voltage cycling between 1 V and 1.80 V for ~1000 h with moderate performance degradation [26]. PEMWE can also provide a glimpse of dynamic operation and a better comparison ground for operational purposes. Papakonstantinou et al. conducted PEMWE for ~800 h and reported performance degradation, which was associated with the chemical instability of the ionomer and membrane under dynamic operation [30]. Alia et al. also reported the performance degradation of PEMWE under dynamic operation [31]. Weiß et al. subjected PEMWE to an on-off cycling operation and reported significant degradation [32]. On-off cycling operations and subjecting the cell to open-circuit conditions without solution feeding harm the stability of electrolyzer cells. Sun et al. introduced Li-ion batteries as intermediatory energy storage systems with renewable energy sources to avoid the adverse effects of intermittency [33]. However, the introduction of Li-ion batteries further complicates the system, making it even more complex. Our previous study found that when the electrolyzer cell was subjected to open-circuit conditions (for 12 h without solution feeding) once in ~100 h of operation, it did not affect the stability of AEMWE [34]. However, degradation is more likely to occur when the cell is subjected to an open-circuit condition > 5 times in 100 h of operation [19]. Herein, we report an operational strategy to avoid such degradation of the AEMWE for a more realistic dynamic operation for coupling with renewable energy sources. The cell was run for ~800 h under an on-off cycling operation regarding an applied electric bias: a constant current of 500 mA cm^{-2} for 5 h followed by a 12 h open circuit. We continuously maintained the supply of the KOH solution to the electrolyzer cell so that the membrane could be protected from dehydration [19]. The ohmic and polarization resistances of the cell were consistently recorded using electrochemical impedance spectroscopy to determine any changes that could occur during operation. This study provides details of operational optimization to cope with dynamic conditions regarding applied electric bias and open-circuit conditions.

2. Experimental

The electrolyzer cell used in this study was purchased from Dioxide Materials, USA. The anode consisted of a porous thin stainless-steel cloth (316L, Bekaert) carrying nanoparticles of $NiFe_2O_4$, whereas the cathode consisted of porous carbon paper (Sigracet 39BC) carrying nanoparticles of NiFeCo. The catalyst loadings of both the anode and cathode were 2 mg cm^{-2} each. Moreover, Sustainion 37-50 was used as the anion-exchange membrane. The electrolyzer had an active area of 6.25 cm^2. The preparation of the electrodes and membrane electrode assemblies (MEAs) is described in [29]. The electrolyzer was operated at 40°C in the on-off cycling mode with an applied electrical bias for ~800 h. For this purpose, a protocol in which the electrolyzer cell was operated under a current density of 500 mA cm^{-2} for 5 h and then left under an open circuit condition for 12 h was designed. The KOH solution was provided to the cell continuously at a rate of 2 mL min^{-1} (this flow rate is sufficient to prevent degradation) whether the cell was under bias or open circuit conditions [19,28,29,34]. This protocol continued until the cells reached approximately 800 h. The operation under a constant current density is called the constant current test. Various techniques like electrochemical characterization, constant current tests, polarization curves, and electrochemical impedance spectroscopy were performed for electrochemical characterization. We measured the polarization curves in a potential window of 1.30 to 2.10 V with a scan rate of 20 mV s^{-1}. Electrochemical impedance spectroscopy was performed at a potential bias of 1.80 V (from 100 kHz to 100 mHz) before and after each constant current test. A Bio-Logic SP 240 potentiostat/galvanostat was used for the electrochemical measurements. After the long-term operation, the conductivity of the membrane was measured using a test fixture developed in-house. An FT/IR 6300 spectrometer (Jasco, Japan)

was used to measure the Fourier transform infrared (FTIR) spectra. Finally, a morphological analysis of the electrodes/MEA was performed by FE-SEM.

3. Results and Discussion

The electrochemical impedance of the electrolyzer cell was recorded at the start of the experiment, as shown in Fig. 1(a), using an equivalent circuit; an inductance was added to the equivalent circuit due to external cablings and connections [35,36]. Impedance was measured at a DC bias of 1.80 V (from 100 kHz to 100 mHz). The ohmic area-specific resistance (ASR) of the cell was the high frequency (9362 Hz) intercept of the real axis. The value was 0.363 Ω cm^2, which arises mainly from membrane resistance. The total ASR of the cell was obtained from a low-frequency (100 mHz) intercept of the real axis (1.156 Ω cm^2). Polarization resistance (non-ohmic ASR) is the difference between the total and ohmic ASRs; its value was 0.793 Ω cm^2. The initial ohmic ASR of the cell was slightly higher than that in our previous studies [19,34,36] because of the lower operating temperature (40°C). However, this value was comparable to those reported in previous studies [22,28,37]. The initial polarization curves (both original and IR-corrected) were measured in a potential window of 1.30 to 2.10 V, as shown in Fig. 1(b). A current density of 685 mA cm^{-2} was recorded at a cell voltage of 1.97 V (IR-corrected).

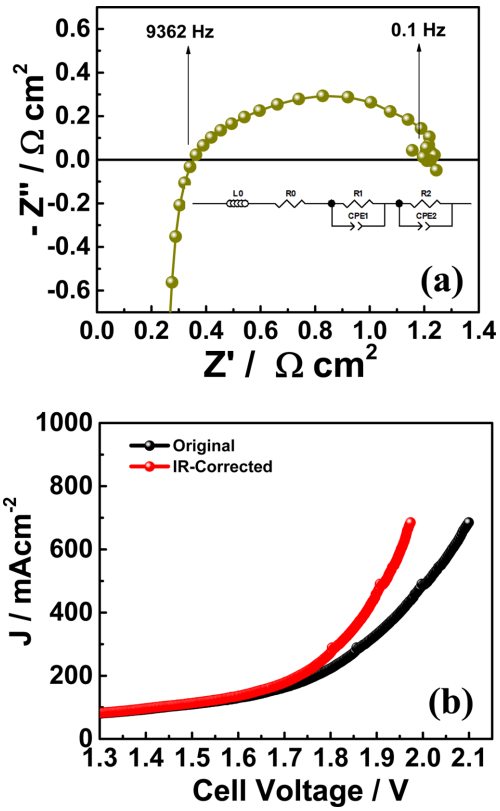

Fig. 1. (a) Nyquist plot of initial impedance spectra measured at 1.80 V. (b) Initial I-V curve measured from 1.30 V to 2.10 V at a scan rate of 20 mV s^{-1}.

According to our test protocol, the electrolyzer cell was subjected to an electric bias (a constant current of 500 mA cm^{-2}) for 5 h, followed by a 12 h open-circuit condition. Fig. 2(a) shows an initial 5 h cell response to the applied current density called "Test-1". After "Test-1", the cell was exposed to an open circuit condition for 12 h. During the open circuit conditions, the KOH solution was provided continuously to the cell to protect the membrane from dehydration. After the open circuit (for 12 h), the electrolyzer cell was subjected to a constant current for the next 5 h. The cell was operated under this protocol until it reached ~800 h. Fig. 2(b) shows the cell voltage variation with respect to time for ~800 h. The 12 h open circuit condition between the consecutive constant current tests in the time duration of 420 to 480 h is shown in Fig. 2(c). Fig. 3(a) shows the electrochemical impedance spectra measured after constant current tests and open circuit conditions in time duration of ~100 to 150 h. The impedance arcs were observed to change with the measurement time. The impedance spectra arc measured after the open circuit condition was significantly larger than that measured after the constant current test. It is worth mentioning that only the low-frequency intercept changed, and the higher-frequency intercept was almost constant. Continuous feeding momentarily increased the non-ohmic resistance while maintaining the membrane under wet conditions; therefore, the ohmic resistance was constant. Continuous solution feeding prevents any increase in the ohmic ASR. The change in ohmic ASR of the cell with time is shown in Fig. 4(a). The star symbol represents the time at which the KOH solution was replaced. The closed symbols correspond to the values of ohmic ASR measured immediately after constant current tests. In contrast, the open symbols correspond to the values of ohmic ASR measured immediately after open-circuit conditions.

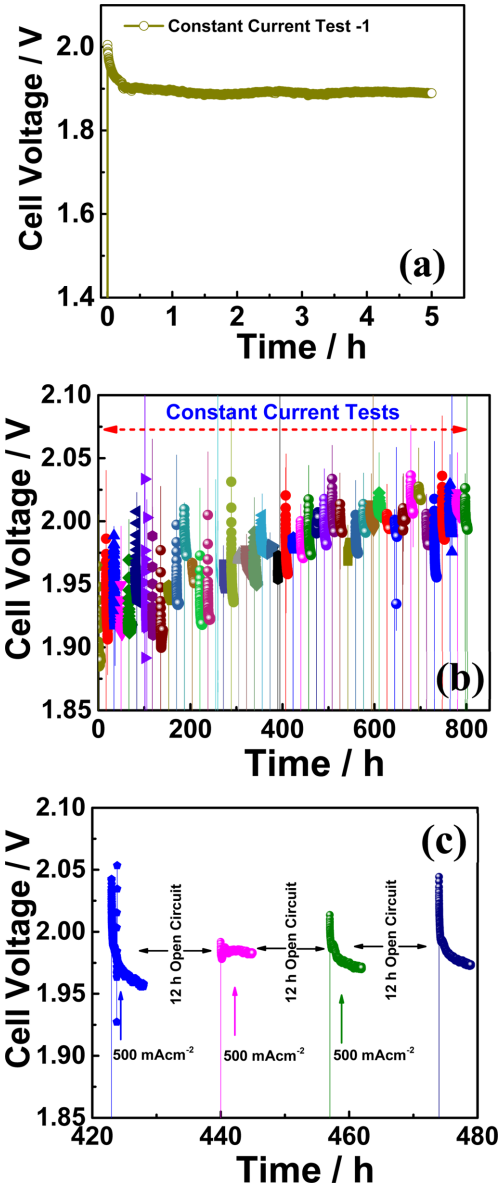

Fig. 2. (a) Cell voltage variation with time under a constant current density of 500 mA cm^{-2} in the initial 5 h, represented as Test-1. (b) Cell voltage variation with time in long-term operation ~800 h. (c) The cell voltage variations with time in 420 h to 480 h duration. A 12 h open circuit condition between the consecutive tests is depicted.

The ohmic ASR values at various stages of the ~800 h operation are listed in Table 1. Such stable values of ohmic ASR are due to the continuous supply of the KOH solution. When the KOH solution was not supplied continuously, the ohmic ASR was reported to

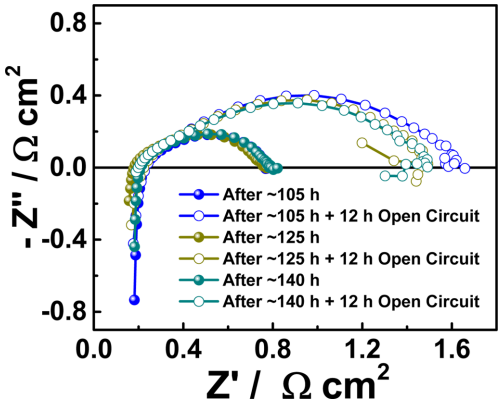

Fig. 3. Nyquist plot of impedance spectra measured after constant current tests and after 12 h open-circuit conditions in time duration of ~100 to 150 h.

Table 1. List of values of ohmic and non-ohmic ASRs at various times during the long-term operation.

	After tests at 500 mA cm^{-2}		After consective open circuit	
Time (h)	Ohmic ASR (Ω cm^2)	Non-ohmic ASR (Ω cm^2)	Ohmic ASR (Ω cm^2)	Non-ohmic ASR (Ω cm^2)
Initial	0.363	0.793	-----	-----
~5 h	0.182	0.272	0.248	0.738
~90 h	0.285	0.757	0.266	0.964
~200 h	0.189	0.619	0.228	1.01
~500 h	0.254	0.654	0.283	0.962
~800 h	0.267	0.764	0.291	1.06

increase irreversibly and lead to performance degradation [19]. However, supplying KOH solution has a momentarily adverse effect on the cell performance, such as an increase in non-ohmic ASR after open circuit conditions (as explained earlier in an increase in the impedance spectra arc). The variation in the non-ohmic ASR of the electrolyzer cell over time is shown in Fig. 4(b). The closed and open symbols correspond to the values measured immediately after constant current tests and open-circuit conditions, respectively. Table 1 shows the non-ohmic ASR values at various stages of the ~800 h operation. The non-ohmic ASR values were higher when measured after the open-circuit condition with solution feeding. However, such an increase in the non-ohmic ASR is reversible, and when the cell is subjected to constant

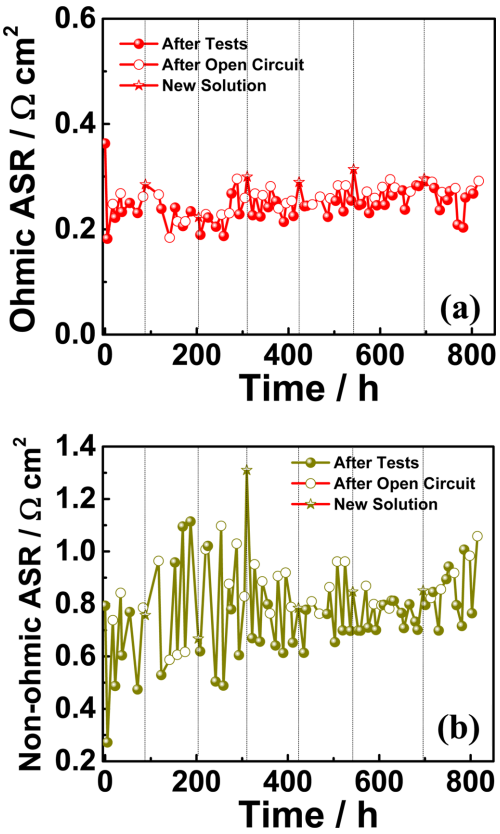

Fig. 4. (a) The variations in ohmic ASR and (b) Non-ohmic ASR of the cell measured with time, the closed and open symbol correspond to measurement immediately after constant current tests and after 12 h open-circuit conditions, respectively while the star symbol and vertical dotted line represent the time when KOH solution was renewed.

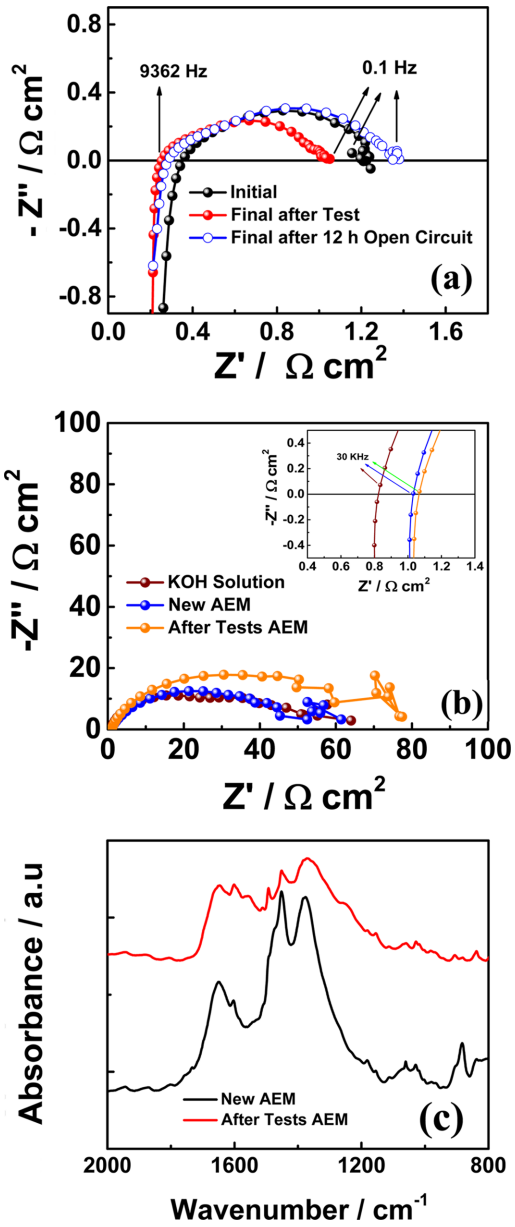

Fig. 5. (a) Nyquist plot of the impedance spectra measured at the start of the experiment, after final test of long-term operation, and after 12 h open circuit condition. (b) Nyquist plots of impedance spectra at 1.80 V of 1 M KOH solution and new and old (after tests) membrane in 1 M KOH solution at 40°C. (c) The FTIR absorbance peaks of the new and after tests membranes.

current tests, the non-ohmic ASR recovers close to the initial value. The impedance spectra of the initial, final after tests, and final after 12 h of the open circuit as a Nyquist plot are shown in Fig. 5(a). The initial value of the non-ohmic ASR is 0.793 Ω cm^2, and the final value after the constant current test is 0.764 Ω cm^2, which are close to each other, indicating that there is no loss of kinetic properties. The final value after a 12 h open circuit is 1.06 Ω cm^2. This value is about ~33% higher than the initial value. However, as Table 1 shows, after every constant current test, the non-ohmic ASR recovers close to the initial value. The increase in non-ohmic ASR was not permanent, and when the electrolyzer cell was run under bias, the performance recovered to almost its initial value. The consistent supply of KOH solution to the cell prevented any unwanted increase in the ohmic ASR of the cell. However, it caused a momentarily reversible increase in the non-ohmic ASR of the cell.

After ~800 h of operation, the electrolyzer was carefully opened to check the conductivity of the membrane and the microstructure of the electrodes. Conductivity measurements of the tested membrane were carried out in a 1 M KOH solution at 40°C. For this purpose, as shown in the Nyquist plots in Fig. 5(b), the impedance of the tested membrane was measured and compared with that of the new membrane. Impedance was measured using a testing fixture developed in-house. Previous work has described the details of the testing fixture and measurement technique [34]. Initially, the ASR of the KOH solution was obtained from the high-frequency intercept (30 kHz) of the real axis and was found to be 0.835 Ω cm^2. The high-frequency intercept of the impedance arc of the new membrane was 1.03 Ω cm^2. This value was the combined ASR of the solution and the new membrane. The ASR value of the new membrane was obtained by subtracting the solution ASR from this value; therefore, the ohmic ASR value of the new membrane was 0.195 Ω cm^2. The ohmic ASR of the tested membrane was similarly obtained as 0.234 Ω cm^2. There is a slight difference between the ASRs of the new and the tested membranes (~0.038 Ω cm^2), which might suggest that the tested membrane was degraded. However, this can be understood as follows: In our previous study, the AEMWE cell was operated for ~1000 h with stable performance. After the long-term operation, the ASRs of the tested and new membranes were measured at 50°C. The ohmic ASR of the tested membrane was 0.208 Ω cm^2, whereas that of the new membrane was 0.182 Ω cm^2. The difference in ASRs was 0.026 Ω cm^2. In the present study, the difference in ASRs (0.038 Ω cm^2) between the tested membrane and the new membrane was comparable to the difference in ASRs (0.026 Ω cm^2) in a previous study for a stable and undegraded membrane [34]. However, this difference in ASRs contrasted with a study in which the membrane was degraded [19]. The ASRs of the tested and new membranes were measured, and the difference was 0.219 cm^2. The difference in ASR between the tested and new membranes was 17 times higher than the difference in ASRs in the present study. Therefore, the membrane retained its ionic conductivity and was stable under on-off cycling for ~800 h. The ohmic ASR value of the tested membrane is also close to the final ASR value, as shown in Fig. 4(a). FTIR analysis was performed on the membrane after the long-term operation (~800 h). The FTIRs of the tested and new membranes were compared, as shown in Fig. 5(c). No new or unknown absorbance peaks were detected, indicating that the membrane was chemically stable during operation. An FE-SEM was used for the morphological analysis of the electrodes. FE-SEM micrographs of the anode GDL, cathode GDL, and membrane are shown in Fig. 6(a)-(f). Fig. 6(a) and (b) show the new anode and cathode GDLs, respectively, before the start of the tests. Fig. 6(c) and (d) show the anode and cathode GDLs after long-term ~800 h tests, respectively. New GDLs were fully covered with thick catalysts, and the GDLs after the long-term tests were void of the catalysts. However, as shown in Fig. 6(e) and (f), the anode and cathode sides of the membrane carried most of the catalyst, respectively. The catalysts remained in contact with the membrane during long-term tests of ~800 h. Consequently, the ohmic ASR was constant, and the non-ohmic ASR recovered to almost its initial value after the cell was subjected to an electric bias. The operational strategy of continuous solution feeding to the AEMWE running under

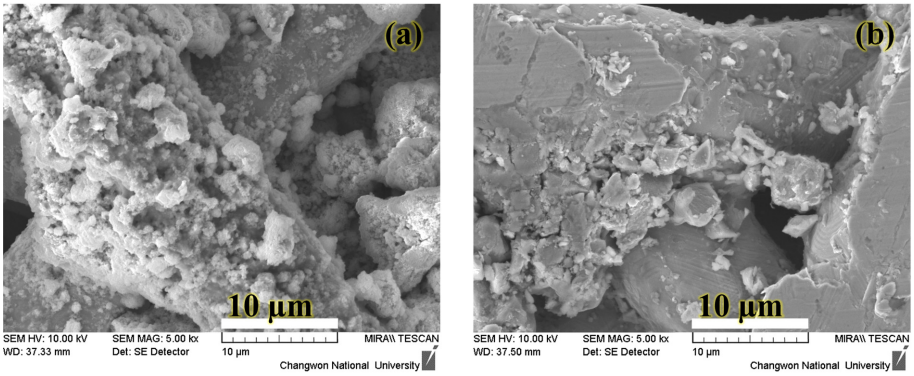

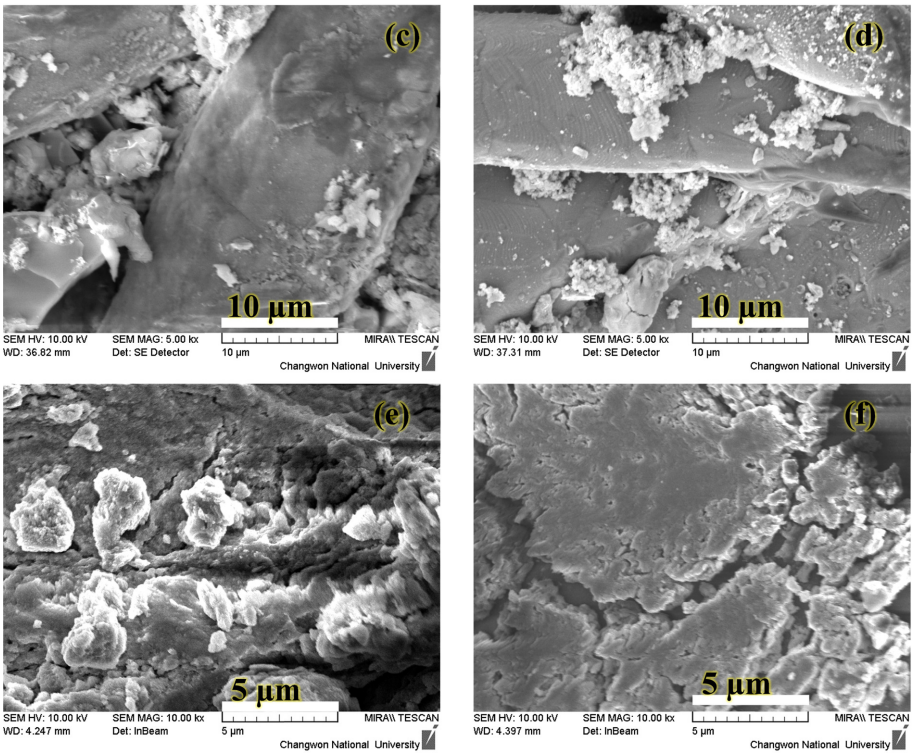

Fig. 6. FE-SEM images of (a) new anode catalysts on the GDL, (b) new cathode catalysts on the GDL, (c) used anode catalysts on the GDL, (d) used cathode catalysts on the GDL, (e) the anode side of the membrane after the test, and (f) the cathode side of the membrane after the tests.

on-off cycling, especially under a prolonged open circuit (12 h), is more beneficial regarding its long-term stability.

4. Conclusions

The stability of the AEMWE cell was investigated under on-off cycling to simulate the electric output of renewable energy sources. A test protocol was designed in which the electrolyzer cell was subjected to an electric bias of 500 mA cm^{-2}, alternating with open-circuit conditions. The KOH solution was supplied continuously to the cell regardless of the electric bias or open circuit. The ohmic ASR of the cell was constant throughout the operation, owing to the continuously fed KOH solution. The polarization resistance increased during the open circuit, though this increase was reversible. Thus, continuous solution feeding to the AEMWE cell under on-off cycling can ensure stable, long-term operation with renewable energy sources.

Acknowledgment

This research was supported by Changwon National University in 2021-2022.

References

[1] J. Ikäheimo, R. Weiss, J. Kiviluoma, E. Pursiheimo, T.J. Lindroos, *Appl. Energy*, **2022**, *305*, 117713.
[2] C. Tolliver, A.R. Keeley, S. Managi, *J. Cleaner Prod.*, **2020**, *244*, 118643.
[3] K. Oshiro, S. Fujimori, *Appl. Energy*, **2022**, *313*, 118803.
[4] M.I. Aydin, I. Dincer, *Energy*, **2022**, *245*, 123090.
[5] P.D. Lund, J. Mikkola, J. Ypyä, *J. Cleaner Prod.*, **2015**, *103*, 437-445.
[6] H. Ritchie, M. Roser, P. Rosado, *Energy*, **2020**, https://ourworldindata.org/energy.
[7] S. Singla, N.P. Shetti, S. Basu, K. Mondal, T.M. Aminabhavi, *J. Environ. Manage.*, **2022**, *302*, 113963.
[8] D. Zhang, H. Zhu, H. Zhang, H.H. Goh, H. Liu, T. Wu, *Energy*, **2022**, *238*, 121774.
[9] A. Skorek-Osikowska, *Int. J. Hydrog. Energy*, **2022**,

47(5), 3284-3293.
[10] H. Mehrjerdi, H. Saboori, S. Jadid, *J. Energy Storage*, **2022**, *45*, 103745.
[11] D. Guilbert, G. Vitale, *Clean Technol.*, **2021**, *3(4)*, 881-909.
[12] C. Santoro, A. Lavacchi, P. Mustarelli, V. Di Noto, L. Elbaz, D. Dekel, F. Jaouen, *ChemSusChem*, **2022**, *15(8)*, e202200027.
[13] M. Mandal, *ChemElectroChem*, **2021**, *8(1)*, 36-45.
[14] D. Li, E.J. Park, W. Zhu, Q. Shi, Y. Zhou, H. Tian, Y. Lin, A. Serov, B. Zulevi, E.D. Baca, *Nat. Energy*, **2020**, *5(5)*, 378-385.
[15] X. Wu, K. Scott, *Int. J. Hydrog. Energy*, **2013**, 38, 3123-3129.
[16] I. Vincent, A. Kruger, D. Bessarabov, *Int. J. Hydrog. Energy*, **2017**,42, 10752-10761.
[17] M. Faraj, M. Boccia, H. Miller, F. Martini, S. Borsacchi, M. Geppi, A. Pucci, *Int. J. Hydrog. Energy*, **2012**, *37(20)*, 14992-15002.
[18] J. Parrondo, V. Ramani, *J. Electrochem. Soc.*, **2014**, *161(10)*, F1015.
[19] A.K. Niaz, A. Akhtar, J.-Y. Park, H.-T. Lim, *J. Power Sources*, **2021**, *481*, 229093.
[20] F. Razmjooei, A. Farooqui, R. Reissner, A. Gago, S.A. Ansar, K.A. Friedrich, *ChemElectroChem*, **2020**, *7(19)*, 3951-3960.
[21] A. Lim, H.-j. Kim, D. Henkensmeier, S.J. Yoo, J.Y. Kim, S.Y. Lee, Y.-E. Sung, J.H. Jang, H.S. Park, *J. Ind. Eng. Chem.*, **2019**, *76*, 410-418.
[22] M.K. Cho, H.-Y. Park, H.J. Lee, H.-J. Kim, A. Lim, D. Henkensmeier, S.J. Yoo, J.Y. Kim, S.Y. Lee, H.S. Park, *J. Power Sources*, **2018**, *382*, 22-29.
[23] J. Parrondo, C.G. Arges, M. Niedzwiecki, E.B. Anderson, K.E. Ayers, V. Ramani, *Rsc Adv.*, **2014**, *4(19)*, 9875-9879.
[24] W.E. Mustain, M. Chatenet, M. Page, Y.S. Kim, *Energy Environ. Sci.*, **2020**, *13(9)*, 2805-2838.
[25] P. Fortin, T. Khoza, X. Cao, S.Y. Martinsen, A.O. Barnett, S. Holdcroft, *J. Power Sources*, **2020**, *451*, 227814.
[26] A. Carbone, S.C. Zignani, I. Gatto, S. Trocino, A. Aricò, *Int. J. Hydrog. Energy*, **2020**, *45(16)*, 9285-9292.
[27] L. Wang, T. Weissbach, R. Reissner, A. Ansar, A.S. Gago, S. Holdcroft, K.A. Friedrich, *ACS Appl. Energy Mater.*, **2019**, *2(11)*, 7903-7912.
[28] J.E. Park, S.Y. Kang, S.-H. Oh, J.K. Kim, M.S. Lim, C.-Y. Ahn, Y.-H. Cho, Y.-E. Sung, *Electrochim. Acta*, **2019**, *295*, 99-106.
[29] Z. Liu, S.D. Sajjad, Y. Gao, H. Yang, J.J. Kaczur, R.I. Masel, *Int. J. Hydrog. Energy*, **2017**, *42(50)*, 29661-29665.
[30] G. Papakonstantinou, G. Algara-Siller, D. Teschner, T. Vidaković-Koch, R. Schlögl, K. Sundmacher, *Appl. Energy*, **2020**, *280*, 115911.
[31] S.M. Alia, S. Stariha, R.L. Borup, *J. Electrochem. Soc.*, **2019**, *166(15)*, F1164.
[32] A. Weiß, A. Siebel, M. Bernt, T.-H. Shen, V. Tileli, H. Gasteiger, *J. Electrochem. Soc.*, **2019**, *166(8)*, F487.
[33] Z. Sun, G. Wang, S.W. Koh, J. Ge, H. Zhao, W. Hong, J. Fei, Y. Zhao, P. Gao, H. Miao, *Adv. Funct. Mater.*, **2020**, *30(27)*, 2002138.
[34] A.K. Niaz, W. Lee, S. Yang, H.-T. Lim, *J. Electrochem. Sci. Tech.*, **2021**, *12(3)*, 358-364.
[35] I. Dedigama, D.J. Brett, T.J. Mason, J. Millichamp, P.R. Shearing, K.E. Ayers, *ECS Trans.*, **2015**, *68(3)*, 117.
[36] A.K. Niaz, J.-Y. Park, H.-T. Lim, *Int. J. Hydrog. Energy*, **2021**, *46(62)*, 31550-31562.
[37] Y. Leng, G. Chen, A.J. Mendoza, T.B. Tighe, M.A. Hickner, C.-Y. Wang, *J. Am. Chem. Soc.*, **2012**, *134(22)*, 9054-9057.